

## Impurity Evaluations of SiO<sub>2</sub> Films Formed on LiNbO<sub>3</sub> Substrates

Hirotohi NAGATA, Hiroki TAKAHASHI, Hiroshi TAKAI<sup>1</sup> and Tamotsu KOUGO<sup>2</sup>

Central Research Laboratories, Sumitomo Osaka Cement Co., Ltd., 585 Toyotomi-cho, Funabashi-shi, Chiba 274, Japan

<sup>1</sup>Tokyo Denki University, Department of Electrical Engineering, 2-2 Kanda-Nishiki-cho, Chiyoda-ku, Tokyo 101, Japan

<sup>2</sup>Machinery and Metallurgy Research Institute of Chiba Prefecture, 6-13-1 Tendai, Inage-ku, Chiba-shi, Chiba 263, Japan

(Received July 21, 1994; accepted for publication December 10, 1994)

SiO<sub>2</sub> films deposited by sputtering (SP) and vacuum evaporation (VE) techniques are commonly used as buffer layers in LiNbO<sub>3</sub>-based devices. The impurity levels in such films are measured as 10<sup>17</sup> to 10<sup>22</sup> atoms/cm<sup>3</sup> for H, Li and Nb ions, which might affect the electrical properties of the devices. The major differences between the SP and VE films are in the density and the hydrogen contents, which possibly influence the *I/V* characteristics of the films and leads to different dc drift phenomena of LiNbO<sub>3</sub> optical modulators made of such layers.

KEYWORDS: SiO<sub>2</sub>, LiNbO<sub>3</sub>, impurities, films

### 1. Introduction

In LiNbO<sub>3</sub> optoelectronic devices, SiO<sub>2</sub> films are generally used as buffer layers between Ti:LiNbO<sub>3</sub> waveguides and metallic electrodes. Consequently, characteristics of the SiO<sub>2</sub> layer influence the device performance. For instance, the mechanical stresses induced by the film formation cause a refractive index fluctuation in the light waveguides, resulting in a shift of the operating point.<sup>1)</sup> Electrical properties of the device, such as the dc drift phenomenon, may be related to the chemical compositions of the buffer layer.<sup>2)</sup> In order to understand the dc drift, which is the key factor in device lifetime,<sup>3)</sup> the SiO<sub>2</sub> structure formed on LiNbO<sub>3</sub> must also be investigated, in addition to the defects and impurities in the LiNbO<sub>3</sub> wafer. It is known that the dc drift phenomena are significantly influenced by the nature of the SiO<sub>2</sub> layer. For instance, the SiO<sub>2</sub> layers formed by different deposition techniques lead to different dc drift results.<sup>4)</sup> Furthermore, the films generally require high-temperature annealing in an oxygen atmosphere,<sup>5)</sup> where diffusion of cations from the LiNbO<sub>3</sub> to SiO<sub>2</sub> is an inevitable problem, possibly leading to the formation of defects at the interface. These cation impurities themselves might be the origin of the dc drift, as well as oxygen defects.<sup>5)</sup> However, there have been no reports on the impurity analysis of SiO<sub>2</sub> films on LiNbO<sub>3</sub> substrates.

This article presents such data for two types of SiO<sub>2</sub> films deposited by sputtering (SP) and vacuum evaporation (VE) techniques. These two kinds of films were examined because different dc drift phenomena were observed for devices with SP and VE SiO<sub>2</sub> buffer layers. Figure 1 shows typical dc drift data for Mach-Zehnder modulators with SP and VE SiO<sub>2</sub> measured at 80°C and a fixed dc bias of 5 V during a 100-day period. The operating point of the SP sample drifts in the suppressing direction of the applied dc bias of 5 V within 1 day of operation. On the other hand, for the VE samples, the initial drift direction is opposite to that of the applied bias, and the drift rate is considerably slow throughout the long-term operation.

### 2. Experimental Results

The films were deposited on the *-z* face of LiNbO<sub>3</sub>

wafers without any waveguides, and some of them were annealed at 600°C for 5 h in flowing wet O<sub>2</sub>.<sup>6, 7)</sup> The samples for *I/V* measurements include the Ti indiffused waveguides. The rf-sputtering depositions (SP) were carried out using a SiO<sub>2</sub> target and an Ar/O<sub>2</sub> (=9/1) mixture at ambient temperature and 0.15 Pa. In the vacuum evaporation depositions (VE), the SiO<sub>2</sub> material was evaporated by electron-beam heating under 3 × 10<sup>-3</sup> Pa of O<sub>2</sub>. The purity of these SiO<sub>2</sub> source materials was 5 N grade.

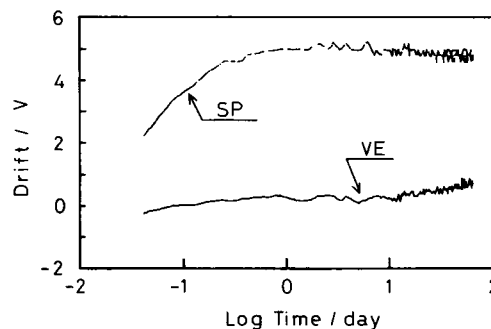


Fig. 1. The dc drift results measured on the Mach-Zehnder optical intensity modulators consisting of the sputtered (SP) and vacuum evaporated (VE) SiO<sub>2</sub> buffer layers. The measurements are carried out at 80°C and fixed dc bias voltage of 5 V during a 100-day period.

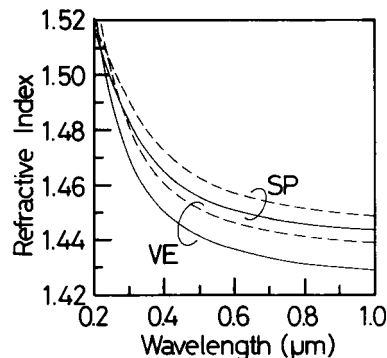


Fig. 2. Refractive indices of the sputtered (SP) and vacuum evaporated (VE) SiO<sub>2</sub> films on LiNbO<sub>3</sub> substrates. The broken and solid lines show the results of as-deposited and annealed films, respectively.

Figure 2 shows the refractive indices ( $n$ ) of the 30-nm-thick films measured by ellipsometry. The  $n$  value of the as-deposited films (broken lines) decreased after the annealing treatment (solid lines) due to a reduction of the oxygen defects in the films.<sup>8)</sup> The smaller  $n$  of the VE-films indicate that the materials prepared by VE had a lower density than those prepared by SP. The relatively low densities of the VE-films were also detected via Si peak intensities in the Rutherford back-scattering (RBS) method.

From the RBS spectra, the major impurities in the films were clarified. Figure 3(a) exhibits the glancing-angle RBS results of the as-deposited (broken line) an annealed (solid line) VE-films and the  $\text{LiNbO}_3$  wafer. The channel positions corresponding to O, Si and Nb are denoted by the arrows in Fig. 3 (a). The  $\text{SiO}_2$  film thicknesses were determined to be about 300 nm from the RBS data and agreed with thicknesses measured by ellipsometry. It was assumed that the high-energy tails of the spectra were the result of the existence of Nb ions throughout the films. Furthermore, the hydrogen content of the annealed films was measured by the hydrogen forward scattering method, as shown in Fig. 3(b). The large peak of the SP-film (solid line) spectrum originated from surface adsorbed molecules. The number of hydrogen atoms was measured as  $1.1 \times 10^{21}$  and  $1.3 \times 10^{22}$  atoms/cm<sup>3</sup> for the SP- and VE-films, respectively. One of the reasons for such a large difference is that the VE-film of lower density could adsorb larger amounts of  $\text{H}_2\text{O}$ .

Finally, secondary ion mass spectroscopy (SIMS) was carried out to investigate Li and Nb contents in the films. Figures 4(a) and 4(b) show the impurity distributions of the SP-films, while (c) and (d) represent those of the VE-films. Results (a) and (c) are for the asdeposited films,

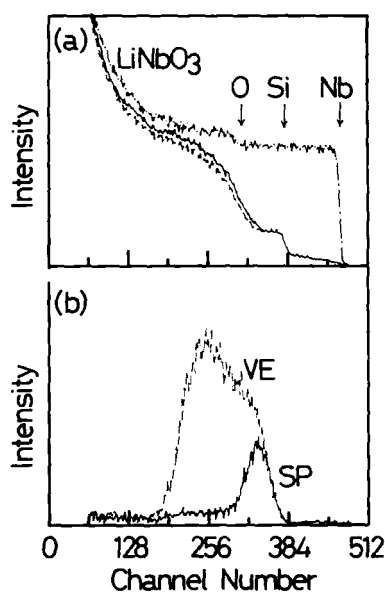


Fig. 3. (a) RBS results of the as-deposited (broken line) and annealed (solid line) vacuum-evaporated (VE)  $\text{SiO}_2$  films on  $\text{LiNbO}_3$  substrates, and the  $\text{LiNbO}_3$  substrate by itself is shown by the dotted line. The angle between the incident 2 MeV  $\text{He}^+$  beam and the detector is  $85^\circ$ . (b) Result of hydrogen forward scattering of the annealed SP (solid line) and VE (broken line) films.

while (b) and (d) are for the annealed films. To check the accuracy of the measurements, a SP- $\text{SiO}_2$  film on a Si substrate was evaluated, where no Nb ( $\ll 10^{15}$  atoms/cm<sup>3</sup>) and  $5 \times 10^{17}$  atoms/cm<sup>3</sup> of Li were detected. From the results, it is evident that Nb ions diffused into the film from the  $\text{LiNbO}_3$  during the film deposition processes. A surprising result is that considerable amounts of Nb ions were incorporated in the VE-film, which is known to be formed via a lower energy process compared to the SP-film.<sup>9)</sup> After annealing, about  $1 \times 10^{17}$  atoms/cm<sup>3</sup> of Nb ions remained in both films. The Nb concentrations of the as-deposited and annealed VE films seem to be different by one order of magnitude (Figs. 4(c) and 4(d)), although they appear to be almost the same in the RBS measurements (Fig. 3(a)). As a possible reason, an uneven concentration depending on the wafer position was considered but the results are yet to be confirmed. Concerning the Li ions, however, since  $5 \times 10^{17}$  atoms/cm<sup>3</sup> of Li were detected, even in the film on the Si substrate, most of the Li incorporated in the films was transferred from the deposition source. For instance, the Li content in the VE source  $\text{SiO}_2$  material was measured as 0.5 ppm. Due to the annealing, Li amounts in the films increased to the order of  $10^{19}$  atoms/cm<sup>3</sup>.

Figure 5 shows the SIMS depth profile through the film/ $\text{LiNbO}_3$  interface of the annealed VE sample. The interface seems indistinct and Si was also detected in the  $\text{LiNbO}_3$  surface. The presence of phases laterally formed at the  $\text{LiNbO}_3$  surface by the interdiffusion phenomena and the concentration of OH ions ( $\text{H}_2\text{O}$ ) may cause fluctuation of the SIMS profile at the interfaces. Furthermore, the RBS spectrum of the same sample could be fitted well to the curve assuming interdiffusion of Nb and Si rather than outdiffusion of Nb only. It is possible that  $\text{SiO}_2$  film formation causes the compositional and structural fluctuations at the interface. Such fluctuations could influence the dc-drifts of the devices, as well as those introduced by the Ti indiffusion process which was previously reported by Minakata.<sup>10)</sup>

As mentioned above, the  $\text{SiO}_2$  films on the  $\text{LiNbO}_3$  contained H, Li and Nb impurities in the range of  $10^{17}$  to  $10^{22}$

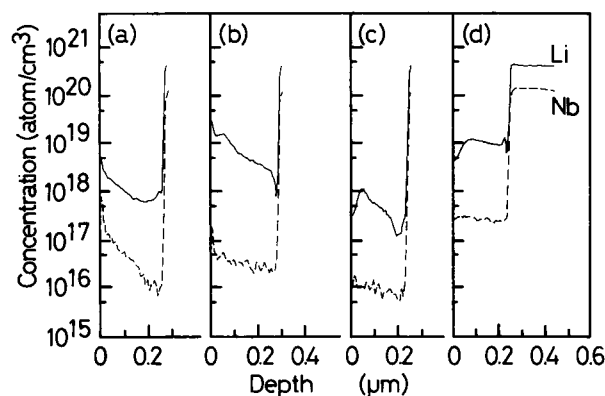


Fig. 4. SIMS results of the as-deposited (a) and annealed (b) SP-films and the as-deposited (c) and annealed (d) VE-films on  $\text{LiNbO}_3$  substrates. The incident beam is  $\text{O}_2^+$  at 6 kV.

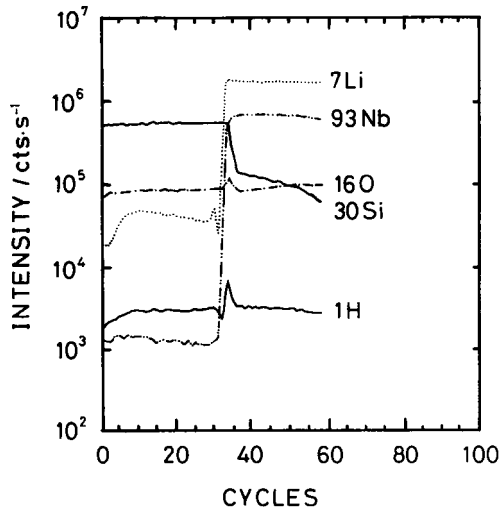


Fig. 5. SIMS results of the annealed VE-film.

atoms/cm<sup>3</sup>. These impurities influenced the electrical characteristics of the films. For instance, H<sup>+</sup> and Li<sup>+</sup> ions were ionic carriers themselves, and when Nb<sup>5+</sup> ions occupied the Si sites of SiO<sub>2</sub> networks, they doped electrons into the SiO<sub>2</sub>. In order to estimate the electrical conductance of such films, *I/V* characteristics between surface electrodes on the Ti:LiNbO<sub>3</sub> optical modulators, including 1 μm-thick-annealed SP- or VE-film, were measured between ±100 V at 29°C and 50% RH using a HP-4140B pA meter. The dimensions of the electrode pair on the SiO<sub>2</sub>/LiNbO<sub>3</sub> were 25 μm gap and 40 mm length perpendicular to the gap. The samples were placed in a shielded box during the measurement. Because the relaxation times of current *I* were on the order of seconds, depending on the sample, the *I* values 2 min after the application of *V* were recorded. The relaxation times at *V* = -5 V, for instance, were 3.5, 11 and 6.2 s for the SP-SiO<sub>2</sub>/LiNbO<sub>3</sub>, VE-SiO<sub>2</sub>/LiNbO<sub>3</sub> and LiNbO<sub>3</sub> samples, respectively. These time-dependent changes in *I* were reversible and after turning off the *V*, the *I* value recovered to the initial (noise) level of |0.5 × 10<sup>-12</sup> A|. Figure 6 shows the Poole-Frenkel plots for the results of the modulators with SP (circles) and VE-SiO<sub>2</sub> (triangles) layers. The *I/V* characteristics of the Ti:LiNbO<sub>3</sub> without the SiO<sub>2</sub> (black marks) showed Ohmic behavior with the resistance of 6.1 × 10<sup>11</sup> Ω. In the samples, including the SiO<sub>2</sub> layers, the Poole-Frenkel behavior was dominant beyond ±20 V, suggesting that the electrons doped by the impurities were the main carriers at these voltages. The carrier density calculated simply from the results at 100 V, with the assumption of 1 μm field penetration and typical mobility of 0.1 cm<sup>2</sup>/Vs for doped glasses,<sup>11)</sup> was on the order of 10<sup>7</sup> to 10<sup>8</sup>/cm<sup>3</sup> which is significantly lower than the impurity densities measured by SIMS, even considering their possible inhomogeneous distribution in the wafer. Such low densities are possibly due to carrier recombinations.

### 3. Discussion and Conclusions

As a source of the dc drift of the LiNbO<sub>3</sub> devices, the

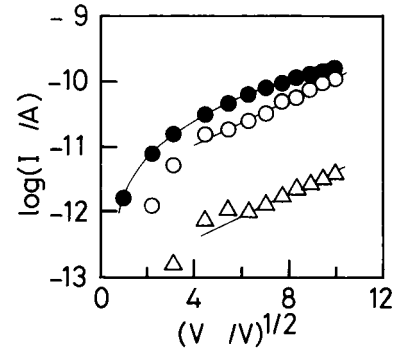


Fig. 6. The Poole-Frenkel plots of *I/V* characteristics for the pair of surface electrodes of Ti:LiNbO<sub>3</sub> modulators with sputtered (white circles) and vacuum-evaporated (white triangles) SiO<sub>2</sub> buffer layers. The black circles are the results of the modulator without any SiO<sub>2</sub> layer.

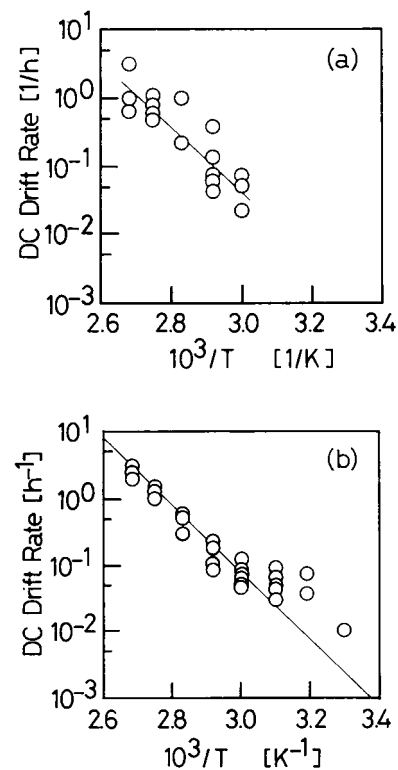


Fig. 7. Arrhenius plots of the positive dc drift rates measured for the Ti:LiNbO<sub>3</sub> optical intensity modulators with VE-SiO<sub>2</sub> buffer layers (a) and with SP-SiO<sub>2</sub> buffer layers (b). The activation energies for (a) and (b) are 0.9 and 1 eV, respectively. The dc drifts are measured at the fixed dc bias of 5 V.

required material parameters for LiNbO<sub>3</sub> crystal itself were recently clarified by Minakata.<sup>10)</sup> In addition to the LiNbO<sub>3</sub>, the electrical characteristics of the SiO<sub>2</sub> buffer layer, due to its structure and compositions, will also affect the dc drift phenomena. The direction of the dc drift was reported to depend on the difference in relaxation times between LiNbO<sub>3</sub> and the SiO<sub>2</sub> layer.<sup>12)</sup> The present results for SiO<sub>2</sub> layers were partly affected by the LiNbO<sub>3</sub> substrate. However, the signs of the relaxation time differences were found to be negative for VE-SiO<sub>2</sub> (3.5–6.2 s) and positive for SP-SiO<sub>2</sub> (11–6.2 s). These signs corresponded to their dc drift behavior, where the device with

VE-SiO<sub>2</sub> drifted first in the opposite direction to the applied dc bias, while the drift direction of the SP-SiO<sub>2</sub> was the same as the applied dc bias (see Fig. 1).<sup>3)</sup> Therefore, the electron conductance in the buffer layers, mentioned here, is believed to affect the early short-term dc drift of LiNbO<sub>3</sub> modulators greatly. The possible origins of such a difference in the relaxation times, leading to the different early drift directions, in the VE and SP films are their density and hydrogen (OH) contents, as observed here.

For the long-term drift, however, other factors should be considered. In the VE-SiO<sub>2</sub> samples, for instance, the activation energies of the drift differed between the early stage toward the negative direction (0.5 eV),<sup>2)</sup> and the following positive one (0.9 eV, see Fig. 7(a)). The activation energy of the positive drifts observed in the SP-SiO<sub>2</sub> modulators was 1 eV (see Fig. 7(b)) and close to that of the positive drifts in the VE-SiO<sub>2</sub> ones, although their drift rates were somewhat different, as shown in the vertical axes of Figs. 7(a) and 7(b). Furthermore, both the SP-SiO<sub>2</sub><sup>6)</sup> and VE-SiO<sub>2</sub><sup>13)</sup> modulators with reduced hydrogen were observed to retain a small drift. These results suggest that rather than the hydrogen content of the SiO<sub>2</sub> layer, that in the LiNbO<sub>3</sub> substrate influences the long-term dc drifts. The influence of the fluctuation of Li, Nb and Si contents at the film/substrate interface on the drift is not clear yet because a specific difference could not be observed for the VE and SP SiO<sub>2</sub> films.

## Acknowledgements

The authors wish to acknowledge Mr. Takano of MST for SIMS measurements and Mr. Suzuki of LEONIX Co., for ellipsometry measurements.

- 1) H. Nagata, K. Kiuchi and T. Sugamata: Appl. Phys. Lett. **63** (1993) 1176.
- 2) H. Nagata and K. Kiuchi: J. Appl. Phys. **73** (1993) 4162.
- 3) H. Nagata, K. Kiuchi, S. Shimotsu, J. Ogiwara and J. Minowa: J. Appl. Phys. **76** (1994) 1405.
- 4) M. Seino, T. Nakazawa, Y. Kubota, M. Doi, T. Yamane and H. Hakogi: *Proc. OFC'92, San Jose, 1992* (Opt. Soc. Am., Washington, 1992) p. 325.
- 5) H. Nishihara, M. Haruna and T. Suhara: *Hikari Shuseki Kairo* (Optic Integrated Circuits) (Ohmsha, Tokyo, 1985) Chap. 7 [in Japanese].
- 6) H. Nagata, J. Ichikawa, M. Kobayashi, J. Hidaka, H. Honda, K. Kiuchi and T. Sugamata: Appl. Phys. Lett. **64** (1994) 1180.
- 7) H. Nagata, K. Kiuchi and T. Saito: J. Appl. Phys. **75** (1994) 4762.
- 8) H. Takahashi, H. Nagata, H. Kataoka and H. Takai: J. Appl. Phys. **75** (1994) 2667.
- 9) S. Yoshida: *Hakumaku* (Thin Films) (Baifukan, Tokyo, 1990) Chap. 1 [in Japanese].
- 10) M. Minakata: IEICE Trans. **J77-C-I** (1994) 194 [in Japanese].
- 11) S. Sakka, T. Sakaino and T. Takahashi: *Garasu Hando Bukku* (Glass Handbook) (Asakura Shoten, Tokyo, 1975) Chap. 12 [in Japanese].
- 12) H. Jumonji and T. Nozawa: IEICE Trans. **J75-C-I** (1992) 17 [in Japanese].
- 13) H. Nagata and J. Nayyer: to be presented at IPR'95 held by Opt. Soc. Am., Dana Point, CA, February 23–25, 1995, ISaB.